Scattering Phenomena of the Propagation Channel at 5.2 GHz on the Baltic Sea

Wei Wang, Gerald Hoerack, Thomas Jost, Ronald Raulefs, Michael Walter and Uwe-Carsten Fiebig
German Aerospace Center (DLR)
Institute of Communications and Navigation
Wessling, Germany

***Abstract*—To investigate the broadband over water-wave propagation channel, the German Aerospace Center conducted a channel sounder measurements where the transmit antenna was mounted on a ship and the receive antenna was located on land. Using this setup, measurements were performed at C-band at 5.2 GHz with a broadband signal of 100 MHz bandwidth. Scattering of the signal due to the roughness of the sea surface is studied and some preliminary results are shown in the paper. The validity of Karasawa's model for a carrier frequency of 5.2 GHz to simulate the scattering phenomenon is shown by evaluating the path loss and power delay profile.**

I. Introduction

Maritime communications today is split into individual systems where each has a single objective in its focus. Non of these systems offer high-data rate with low latency as used on land in cellular mobile radio systems. Alternative systems offering high-data rates are satellite based systems which are rather expensive and limited by serving only a small number of users in the coverage zone with promised data rates. Therefore, high-data rate systems could combine the demand of multiple systems, and would even allow new applications with a higher demand of bandwidth, such as remote operating ships or offshore activities. In the $5-6\,\mathrm{GHz}$ band a spectrum is identified by the European Conference of Postal and Telecommunications Administrations (CEPT) in conjunction with European Telecommunications Standards Institute (ETSI) to offer maritime broadband radio links in the near future. Therefore, it is essential to understand the broadband radio link over sea.

To develop new algorithms for future communication and navigation systems on ship, it is essential to understand the wireless propagation characteristics of the sea surface scattering. One possible approach to gain knowledge about the wireless propagation channel is to conduct channel measurement campaigns. In the recent years some channel measurement campaigns were performed in maritime scenarios [1], [2], [3], [4], [5], [6], [7]. However, these measurements were conducted with small bandwidth (maximum $20\,\mathrm{MHz}$) and therefore, with low delay-resolution. Also the influence of the height of the transmit and/or receive antennas on the propagation channel has not been fully investigated. Furthermore, there is no terrestrial based maritime channel model suitable for simulations of wideband communication and/or navigation applications.

To better understand the propagation over sea, a broadband channel measurement campaign in a maritime scenario was performed by the Institute of Communications and Navigation of the German Aerospace Center (DLR) on the Baltic sea in March 2014. The channel measurement was conducted with a MEDAV RUSK channel sounder operating at the carrier frequency $5.2\,\mathrm{GHz}$ with bandwidth of $100\,\mathrm{MHz}$. On both transmitter and receiver, Rubidium clocks are used to provide stable frequency standards for both sides. The drifts of the Rubidium clocks were monitored by using line-of-sight (LoS) calibration as well as by using Global Positioning System (GPS) receivers. In this paper, we present details of the channel measurement campaign and some preliminary results focusing on the scattering phenomena.

II. Channel Measurements

DLR performed measurements on the Baltic sea in March 2014 as described in [8]. The measurements were accomplished using a Medav RUSK-DLR channel sounder at operating center frequency $5.2\,\mathrm{GHz}$ (C-band). The receiver was located on land in Warnemuende, Germany. Two sites on land were considered for receiver location: the light house Warnemuende and the highest building of the city as visualized in Fig. 1. For the light house Warnemuende, the receive antenna was mounted on a tripod located on two different heights, around $21.6\,\mathrm{m}$ and $32.9\,\mathrm{m}$ above the mean sea level. For the highest building, the receive antenna was mounted on a tripod located on two different heights, around $32.3\,\mathrm{m}$ and $48\,\mathrm{m}$ above the mean sea level. The position of the receive antenna was measured by a GPS receiver.

Fig. 1: Two sites used as the receiver locations on land.

Fig. 2: View of the ship "Rosenrot" where the transmit antenna was mounted on.

The transmitter was located on a ship from the German Federal Administration of Water- and Shipping (WSV). A $47\,\mathrm{dBm}$ spread spectrum signal — in particular a multitone signal — at center frequency $5.2\,\mathrm{GHz}$ with a bandwidth $B = 100\,\mathrm{MHz}$ was transmitted by an onmi-directional antenna mounted on the mast of the ship as shown in Fig. 2. The periodic signal was linearly polarized with a time duration of $T_p = 12.8\,\mu\mathrm{s}$ per period. During the measurement, the ship was moving with a speed ranging from $1\,\mathrm{m/s}$ to $5\,\mathrm{m/s}$. Fig. 3 visualizes an example of the ship traveling route when the receiver was located on the light house. In this scenario, the maximum distance between the transmitter and the receiver is around $12\,\mathrm{km}$. The position of the transmit antenna was measured by a GPS receiver.

Table I lists the summarized setup of the channel measurement campaign. During the measurement, the receiver saved channel impulse response (CIR) snapshots $h(t_k, \tau_n)$, where $t_k = k \cdot t_g$, with $k = 1, 2 \ldots$, is the time index of the measured CIR snapshots and $\tau_n = n \cdot \tau_\Delta$, with $n = 0, \ldots, N-1$, is the delay of sample n. The signal bandwidth B determines the

Fig. 3: Route of the ship visualized by the red lines when the receiver was located on the light house.

Fig. 4: 2×16 antenna array used during the measurement campaign.

CIR delay resolution $\tau_\Delta = \frac{1}{B}$. The signal period T_p of the transmitted signal determines the maximum time length of the channel impulse response snapshot. As a result, a maximum detour propagation distance of $3.8\,\mathrm{km}$ larger than the distance between the transmitter and the receiver can be measured by the channel sounder. Two different types of measurements were conducted: single-input single-output (SISO) and the single-input multiple-output (SIMO). In the former type of measurement, an omni-directional antenna was used at the receiver. In the latter type of measurement, a circular antenna array with 2×16 elements were used as visualized

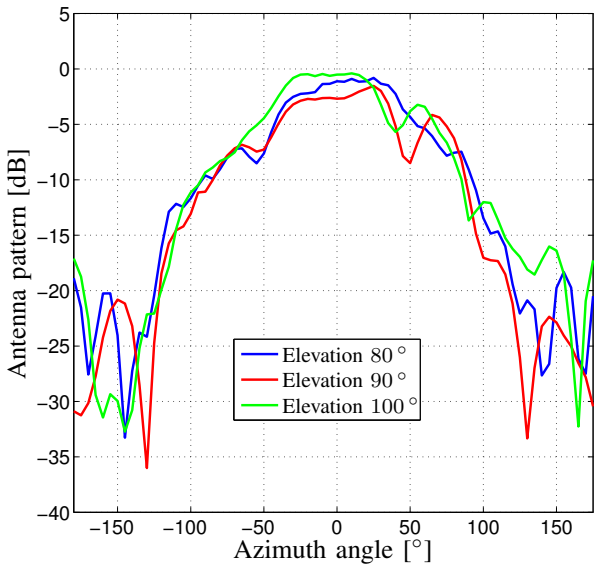

Fig. 5: Measured antenna pattern of a single antenna element.

Parameter	Value
RF centre frequency	5.2 GHz
Bandwidth B	100 MHz
Number of sub-carriers N	1281
Sub-carrier spacing Δf	78.125 kHz
Transmit power	47 dBm
Signal period T_p	12.8 μs
Block repetition rate	18.432 ms
Transmitter antenna	Omni-directional (V-polarized)
Receiver antenna	Omni-directional (V-polarized) and Dual-polarized array
Ship speed	$< 5\,\mathrm{m/s}$

TABLE I: Channel sounder settings.

in Fig. 4. Each antenna element was dual polarized and, therefore, in total 64 channels were measured. To obtain the angle dependent complex gain of the antenna array, a calibration of the antenna array has been conducted in an anechoic chamber. Fig. 5 shows an example of obtained antenna pattern for a single antenna element.

To achieve a good synchronization between the transmitter and the receiver, two Rubidium clocks were used on each side. In the beginning of every measurement day, a reference measurement, where the transmitter had a clear LoS to the receiver, was performed to measure the time offset between both clocks. It has been reported that the Rubidium clock is short term stable but not in the long term case. The Rubidium clock used in the measurement is well known for its short term stability ($3{\cdot}10^{-12}/100$s) and also the accuracy of the clock is high ($< 5{\cdot}10^{-11}$). Thus, for each CIR measurement the phase drift caused by clocks are ignorable. To compensate the clock drift during the measurement, the clock offsets of both clocks compared to GPS time were monitored and recorded. Therefore, the relative drift between both clocks can be obtained by post processing of the time information. A more detailed description to the clock monitoring by using GPS measurements can be found in [9].

III. Scattering Phenomenon on Sea Surface

Apart from the direct propagation between the transmitter on the ship and receiver on land, the interactions between the sea surface and the signal need to be considered as visualized in Fig. 6. First, the signal propagates along a specular path which is reflected on the sea surface. The interaction point of the reflected path can be determined according to the geometry relation of the transmitter, receiver and sea level. The amplitude of the reflected path depends on environmental conditions (e.g., the salinity of the water, temperature, smoothness of the sea surface) and can be calculated according to Karasawa's model [10], [11] as

$$\alpha_{\mathrm{ref}} = \frac{\sqrt{P_t G_t G_r}\,\Gamma\left(\theta_i\right)\lambda e^{-2(kh_0\cos\theta_i)^2} e^{-j2\pi\frac{d_1+d_2}{\lambda}}}{4\pi\left(d_1+d_2\right)}, \tag{1}$$

where P_t is the transmitted power, d_1 and d_2 are the transmitter-scatterer distance and receiver-scatterer distance, respectively, θ_i is the incident angle of the signal on the sea, $\Gamma\left(\theta_i\right)$ is the reflection coefficient depending on the incident angle θ_i of the signal on the sea surface, $k = \frac{2\pi}{\lambda}$ is the wavenumber, λ is the wavelength, h_0 is the root mean square sea surface height, and G_t and G_r are gains of transmit antenna and receive antenna, respectively[1].

Apart from the reflected path, the signal may also be scattered by the irregular sea surface. The scattering affect below 2 GHz has been widely studied in past years [10], [11]. The surface of the sea may be divided into several tiles with small sizes, within which a scattered component is calculated. The amplitude of individual scattering path is given as [10], [11]

$$\alpha_{\mathrm{sca}} = \frac{\sqrt{P_t G_t G_r \Delta A \sigma_0\left(\theta_i,\theta_s\right)}\lambda S\Gamma\left(\theta_i\right) e^{-j2\pi\frac{d_1+d_2}{\lambda}}}{(4\pi)^{\frac{3}{2}}\, d_1 d_2}, \tag{2}$$

where S is the shadowing factor, ΔA is the tile area and $\sigma_0\left(\theta_i,\theta_s\right)$ is the normalized radar cross section of

[1]Practically, the antenna gain depends on the angle θ_i. For notation convenience the angle dependent term is discarded.

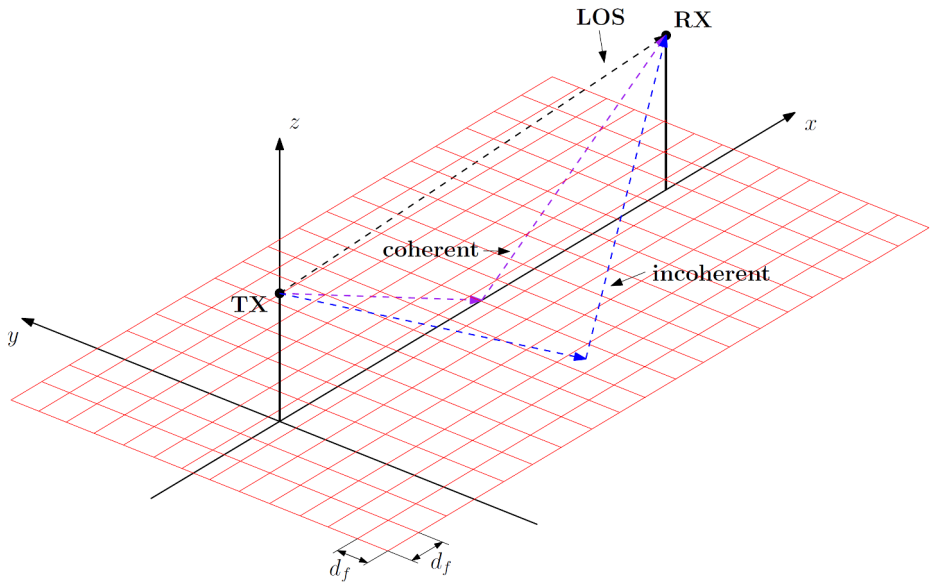

Fig. 6: Geometry of the scattering model.

individual tile depending on the incident angle θ_i and the outgoing scattering angle θ_s and is given as

$$\sigma_0(\theta_i, \theta_s) = \begin{cases} \frac{u^4}{\beta^2} \sec^4\gamma e^{-u^2\left(1+\frac{\tan^2\gamma}{\beta^2}\right)} & u^2 \ll 1 \\ \frac{1}{\beta^2} \sec^4\gamma e^{\frac{\tan^2\gamma}{\beta^2}} & u^2 \gg 1 \end{cases} \tag{3}$$

where roughness parameter $u = kh_0(\cos\theta_i + \cos\theta_s)$ and $\beta = \frac{2h_0}{l_0}$ with sea surface correlation length l_0, and γ given as

$$\gamma = \tan^{-1}\left(\frac{\sqrt{\sin^2\theta_i - 2\sin\theta_i\sin\theta_s\cos(\phi_s) + \sin^2\theta_s}}{\cos\theta_s + \cos\theta_s}\right) \tag{4}$$

with the azimuth angle of the scattering path ϕ_s. Currently Karasawa's model has been mainly focused on carrier frequency below 3 GHz. In the following, some preliminary results for a carrier frequency of 5.2 GHz are presented.

IV. Preliminary Results

We present preliminary results based on the SIMO measurement with the 2×16-element dual-polarized antenna array. So far we considered the vertically polarized channels of the antenna elements in this section. Therefore, we are focusing on the vertical polarization on both transmitter and receiver sides. In order to suppress and mitigate the influence of multipath components (MPCs) caused by physical objects on the land, we use those antenna elements whose main beam direction (i.e., the $0\,^\circ$ direction in Fig. 5) is pointing to the ship route during the measurement campaign.

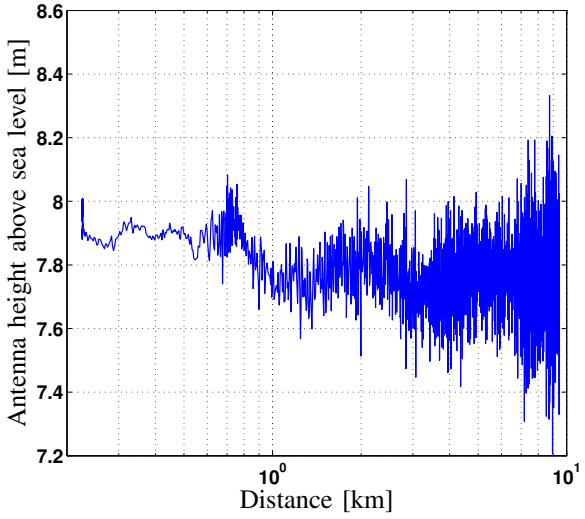

Fig. 7: The measured ship-mounted antenna height above sea level by using GPS.

The obtained time variant height (above the sea level) of the antenna mounted on the ship is shown in Fig. 7. In the beginning, the ship was moving in the harbor and, therefore, the variation of the height is small. While the ship moves on the open sea, the height of the antenna varies more due to the ocean waves. The dynamic height is used to calculate the LoS path, specular path and the scattered paths.

Fig. 9 shows separately the different signal components simulated by the scattering model. The solid black

line represents the LOS signal, which corresponds to the free space loss. The green line shows the model result for a two-ray propagation (LOS and specular reflection), which is similar to the REL model. As shown in Fig. 9, the superposition of all three components (i.e. the total received power) is illustrated in red. The interesting parts are the trends of coherent and incoherent component. The behavior of both can be best explained by the roughness parameter u. Since the electromagnetic wavelength is fixed, u depends on the RMS surface height h_0, the angle of incidence θ_i and the scattering angle θ_s. For a perfectly smooth sea (i.e. $h_0 = 0$ and $u = 0$) the coherent component reaches a maximum and the incoherent component decreases to zero. This would result in a simple two-ray propagation without random signal variations, where the coherent component only depends on the Fresnel reflection coefficient. With growing h_0 the coherent component is decreased and the diffuse scattering increases.

Since h_0 is assumed to be constant during the simulations, the roughness parameter is only affected by the angles θ_i and θ_s, where u has its maximum for $\theta_i = \theta_s = 0$ (vertical incidence and reflection) and it decreases with increasing angles θ_i and θ_s (i.e. decreasing elevation angles). Therefore, the coherent component is very weak at short distances. For increasing TX-RX-distances the specular reflection becomes stronger and it exceeds the incoherent component between 1 and 2 km (cf. Fig. 9). Above this distance the constructive and destructive interferences between direct LoS signal and coherent component become dominant. At the same time the diffuse scattering looses the significance with increasing separation of transmitter and receiver. Fig. 9 visualizes the scattering coefficient σ_0. The distance between transmitter and receiver is 500 m in x-direcion. σ_0 is dimensionless and is represented linearly. It is important to note, that x- and y-axis are not equally scaled. This means, scattering mainly occurs within a narrow and elongated region between TX and RX.

Fig. 10 visualizes the received power during the measurement where the receiver was located on the light house at a height of 32.9 m above the sea level. As a comparison, the ITU maritime path loss model [12] proposed for carrier frequencies below 3 GHz was also evaluated. Also the predicted power by using the theory in Section III is visualized in the figure, where the LoS path, the specular path and the scattered paths on the sea surface are considered. It is worth to note that the fast power variations when only LoS and specular paths are considered is caused by the dynamic height of the ship. The scattering affect on the sea results in additional fast power variation.

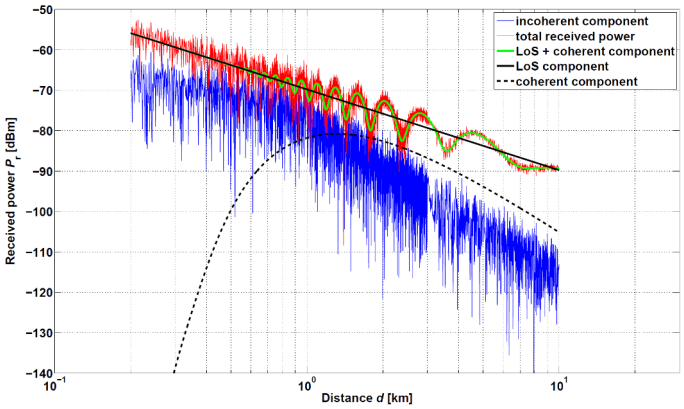

Fig. 8: Separated components for lighthouse/upper floor (32.9 m above MSL).

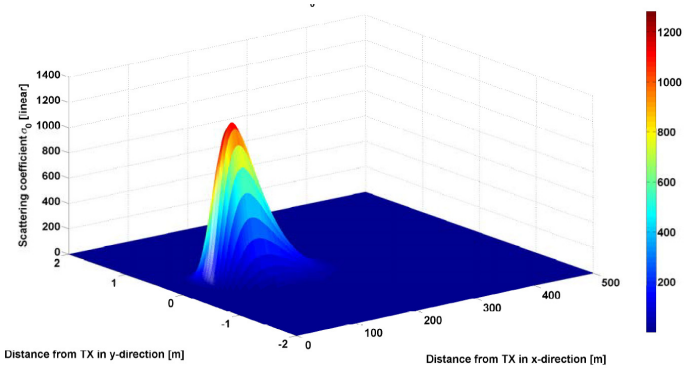

Fig. 9: Scattering coefficient σ_0 for a distance of 500 m between transmitter and receiver.

V. Conclusion and Future Work

To investigate the broadband over waterwave propagation channel, the German Aerospace Center conducted a broadband channel sounder measurements where the transmit antenna was mounted on a ship and the receive antenna was located on the land. Using this setup, measurements were performed for C-band at 5.2 GHz with a broadband signal of 100 MHz bandwidth. As an important propagation phenomenon over the sea, the scattering affect is studied using Karasawa's model in the paper. The study in this paper shows that Karasawa's model still shows a validity for the propagation at carrier frequency 5.2 GHz. Further improvement can be done in terms of using the physical optic method by incorporating the full dimension information of the sea surface (i.e., the norm of individual tile).

Acknowledgement

We would like to thank German Federal Waterways and Shipping Administration (WSV) providing the ship

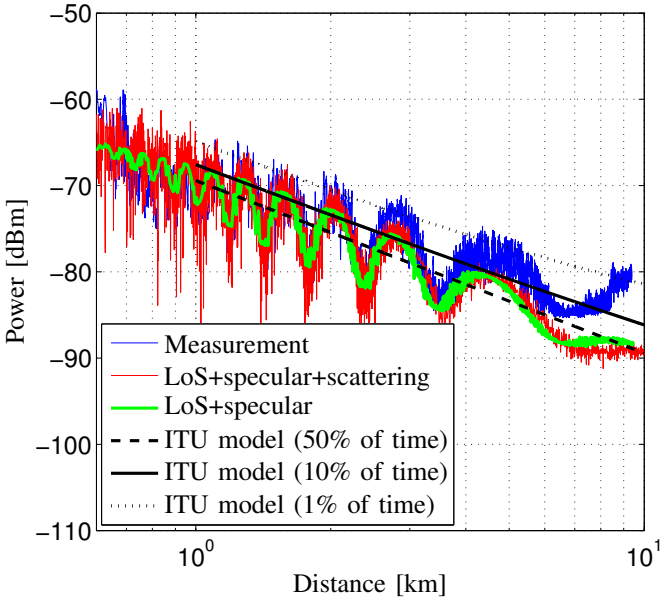

Fig. 10: The measured received power level compared with the simulated power with ITU models and scattering model. The percentages of time represent that the power levels exceed for 50%, 10% and 1% of time.

Rosenort and Prof. Fernando Perez-Fontan for fruitful discussions.

Financial Support

The research leading to these results has been carried out under the framework of the project 'R&D for the maritime safety and security and corresponding real time services'. The project started in January 2013 and is led by the Program Coordination Defence and Security Research within the German Aerospace Center (DLR).

References

[1] K. Yang, T. Roste, F. Bekkadal, K. Husby, and O. Trandem, "Long-Distance Propagation Measurements of Mobile Radio Channel over Sea at 2 GHz," in *Vehicular Technology Conference (VTC Fall), 2011 IEEE*, Sept 2011, pp. 1–5.

[2] K. Yang, A. Molisch, T. Ekman, and T. Roste, "A Deterministic Round Earth Loss Model for Open-Sea Radio Propagation," in *Vehicular Technology Conference (VTC Spring), 2013 IEEE 77th*, June 2013, pp. 1–5.

[3] J. Joe, S. Hazra, S. H. Toh, W. M. Tan, J. Shankar, V. D. Hoang, and M. Fujise, "Path Loss Measurements in Sea Port for WiMAX," in *Wireless Communications and Networking Conference, 2007.WCNC 2007. IEEE*, March 2007, pp. 1871–1876.

[4] J. Joe, S. Hazra, S. H. Toh, W. M. Tan, and J. Shankar, "5.8 GHz Fixed WiMAX Performance in a Sea Port Environment," in *Vehicular Technology Conference, 2007. VTC-2007 Fall. 2007 IEEE 66th*, Sept 2007, pp. 879–883.

[5] K. Maliatsos, P. Constantinou, P. Dallas, and M. Ikonomou, "Measuring and modeling the wideband mobile channel for above the sea propagation paths," in *Antennas and Propagation, 2006. EuCAP 2006. First European Conference on*, Nov 2006, pp. 1–6.

[6] J. Reyes-Guerrero and L. Mariscal, "5.8 GHz Propagation of Low-Height Wireless Links in Sea Port Scenario," *Electronics Letters*, vol. 50, no. 9, pp. 710–712, Apr. 2014.

[7] Y. Lee, F. Dong, and Y. Meng, "Near Sea-Surface Mobile radiowave Propagation at 5 GHz: Measurement and Modeling," *Radioengineering*, vol. 23, no. 3, pp. 824–830, sep 2014.

[8] W. Wang, R. Raulefs, T. Jost, A. Dammann, C. Gentner, and S. Zhang, "Ship-to-Land Broadband Channel Measurement Campaign at 5.2 GHz," in *The MTS/IEEE Oceans*, St. John's, Canada, September 2014.

[9] N. Schneckenburger, B. Elwischger, B. Belabbas, D. Shutin, M. Circiu, M. Suess, M. Schnell, J. Furthner, and M. Meurer, "Navigation performance using the aeronautical communication system LDACS1 by flight trials," in *European Navigation Conference*, April 2013.

[10] D. Barrick, "Rough Surface Scattering Based on the Specular Point Theory," *IEEE Transactions on Antennas and Propagation*, vol. 16, no. 4, pp. 449–454, Jul. 1968.

[11] Y. Karasawa and T. Shiokawa, "Characteristics of L-Band Multipath Fading due to Sea Surface Reflection," *IEEE Transactions on Antennas and Propagation*, vol. 32, no. 6, pp. 618–623, Jun. 1984.

[12] ITU-R Recommendation P.1546-2, "Method for point-toarea predictions for terrestrial services in the frequency range 30 MHz to 3000 MHz," , Sep. 2005.